Distinct profiles of myelin distribution along single axons of pyramidal neurons in the neocortex.

(Article begins on next page)

19 October 2024

Distinct profiles of myelin distribution along single axons of pyramidal neurons in the neocortex

Giulio Srubek Tomassy[1], **Daniel R. Berger**[2,3], **Hsu-Hsin Chen**[1], **Narayanan Kasthuri**[2], **Kenneth J. Hayworth**[2], **Alessandro Vercelli**[4], **H. Sebastian Seung**[3,5], **Jeff W. Lichtman**[2], and **Paola Arlotta**[1,*]

[1]Department of Stem Cell and Regenerative Biology, Harvard University, 7 Divinity Avenue, Cambridge MA 02138

[2]Department of Molecular and Cellular Biology, Harvard University, 52 Oxford Street, Cambridge, MA 02138

[3]Department of Brain and Cognitive Sciences, Massachusetts Institute of Technology, 43 Vassar Street, Cambridge, MA 02139

[4]Neuroscience Institute Cavalieri Ottolenghi, Neuroscience Institute of Turin, Corso M. d'Azeglio 52, Turin, Italy10126

Abstract

Myelin is a defining feature of the vertebrate nervous system. Variability in the thickness of the myelin envelope is a structural feature affecting the conduction of neuronal signals. Conversely, the distribution of myelinated tracts along the length of axons has been assumed to be uniform. Here, we traced high-throughput electron microscopy (EM) reconstructions of single axons of pyramidal neurons in the mouse neocortex and built high-resolution maps of myelination. We find that individual neurons have distinct longitudinal distribution of myelin. Neurons in the superficial layers displayed the most diversified profiles, including a new pattern where myelinated segments are interspersed with long, unmyelinated tracts. Our data indicate that the profile of longitudinal distribution of myelin is an integral feature of neuronal identity and may have evolved as a strategy to modulate long-distance communication in the neocortex.

Myelin plays critical roles in enabling complex neuronal function, including learning and cognition, and abnormal myelination is associated with neurological disorders and mental illnesses(1, 2). Given the importance of myelin for network behavior, realistic models of structure-function relationship in the central nervous system (CNS) must be built in consideration of myelin structure and distribution as fundamental elements. Among all myelinated axons the thickness of the myelin sheath varies greatly and it is a major determinant of the speed of impulse propagation(1). However, structural features other than myelin thickness have the potential to contribute to the establishment and modulation of conduction velocity and to network behavior. In particular, the alternating sequence of nodes and internodes along each axon could affect conduction speed.

---

[*]correspondence should be addressed to P.A. at paola_arlotta@harvard.edu.
[5]Current address: Princeton Neuroscience Institute, Princeton University, Princeton, NJ 08544

High-resolution maps of myelin distribution along individual axons are not currently available. Notably, it is not known whether different neurons are endowed with signature patterns of longitudinal myelination. This analysis has been hampered by the technical difficulty of tracing single, long, winding axons through the complex milieu of the CNS, a task that requires EM serial reconstructions of large volumes of tissue. Fortunately however large EM datasets that allow analysis of myelin are beginning to be available (3, 4). Here, using the neocortex as a prominent model of neuronal diversity we traced the distribution of myelin along a large set of individual pyramidal neuron axons to understand whether myelin properties differ among different types of neurons. Pyramidal neurons occupy different cortical layers, have distinct molecular and long-distance connectivity properties and compute the highest-level cognitive, sensory and motor functions of the mammalian CNS (5, 6).

We first assessed the distribution of myelin within the adult mouse somatosensory (S1) cortex. Immunohistochemistry for myelin basic protein (MBP) and the transcription factor CUX1 (a marker of layers II–IV pyramidal neurons(7)) showed that the lowest levels of myelin correspond to layer II/III, while layer IV neurons reside in an intermediate domain and layers V and VI are the most densely myelinated (Fig. 1A). The same pattern of myelin distribution was evolutionarily conserved in primates, including humans, and it is maintained in the aged cortex (Fig. S1). To determine whether a correlation exists between this myelin gradient and the longitudinal deposition of myelin along axons of different neurons, we performed Golgi-Cox staining, which labels neuronal somas, dendrites and unmyelinated axons (but not the myelinated segments of axons(8)). We found that the distance between the axon hillock and the beginning of the first internode, which we refer to as pre-myelin axonal segment (PMAS), was inversely correlated with the distance of the neuron soma from the pia (Fig. 1B). This result suggests that neurons in different layers display different profiles of longitudinal myelination.

In order to follow individual axons at higher resolution and over long distances, we used two high-throughput EM serial reconstruction datasets spanning large volumes of the adult neocortex. The first dataset spans a $500\times1000\times61~\mu m^3$ volume of mouse somatosensory (S1) cortex from layer I to VI and was sectioned at 30 nm thickness. Every 8th section was imaged at a resolution of 30nm, resulting in an image stack with $30\times30\times240$ nm per pixel (see Methods and Fig. S2A). The second dataset spans a $450\times350\times54~\mu m^3$ volume of mouse visual cortex (V1) from layer I to the upper margin of layer IV (9) and is available for download at (http://www.openconnectomeproject.org). In order to trace individual axons, we used VAST - Volume Annotation and Segmentation Tool (see Methods) - to reconstruct single neurons, their processes and associated myelin over long distances (Movie S1). These tracings can all be reproduced using the TrakEM2 plug-in of the Fiji framework(10).

We traced 38 axons from neurons located in layers III through VI of the S1 dataset. Neurons in layer II/III could not be traced in the S1 dataset due to slice folding in the outer-most part of the cortex. To map myelin distribution in these more superficial layers, we therefore employed the V1 dataset and traced a total of 22 additional neurons located in layer II/III (Fig. 2 and Table S1). A movie showing the reconstruction and tracing of a representative neuron from layer II/III is shown in Movie S1. First, we normalized the length of the

myelinated tracts on each axon to the total axonal length traced. In agreement with MBP distribution we found that axons in layer V and VI have a total myelin coverage higher than axons in layers II/III (layer V-VI, 63.0±5.6% coverage, n=12; layer III–IV, 56.7±4.2% coverage, n=26; layer II/III, 37±4.3% coverage, n=22; mean±s.e.m., p 0.001; Fig. S2A,B and Movies S2 and S3). In addition, as indicated by the Golgi-Cox staining, the PMAS length of layer III and IV neurons was significantly longer than that of layer V and VI neurons (layer III–IV, 48.4±3.5 μm, n=26; layer V–VI; 33.7±2.4 μm, n=12; mean±s.e.m., p= 0.00017, Fig. 1C).

Notably, the majority of the neurons traced in layer II/III displayed a pattern of longitudinal myelination that had never been described before in the CNS. 17 out of 22 neurons had myelinated axonal tracts of variable lengths (ranging between 18.28 μm and 57.36 μm), which were intercalated with long unmyelinated segments (up to 55.39 μm in length) (Fig. 2 and Fig. S3). These myelin gaps were longer than typical nodes of Ranvier (1–2 μm)(1, 2). In contrast to layer II/III neurons, 9 out of 12 neurons traced in layers V–VI presented long myelinated tracts interrupted by nodes of Ranvier, with the exception of three neurons that showed short myelin gaps (7.3, 16.4 and 20.4 μm) (Fig. 1C, red neuron and Fig. S4). This suggests that intermittent myelination is a signature of layer II/III pyramidal neurons and that not all neurons display the same longitudinal profiles of myelination. Layer II/III pyramidal neurons are involved in elaborate cortical activities and exhibit a higher degree of molecular and electrophysiological heterogeneity as compared to layer V and VI neurons(11). The observed structural heterogeneity might contribute to the functional diversity of this complex neuronal population and be important when modeling neuronal function and network behavior in the CNS.

In addition to the 17 neurons with intermittent myelination, we found that three neurons in layer II/III had exceptionally long PMAS (142.5, 121.6 and 101.2 μm; Fig. 2 and Fig. S3). Finally, we found two neurons whose axons were unmyelinated until the lower border of the dataset (for a total distance of 208.4 μm and 193.1 μm, respectively) (Fig. 2 and Fig. S3). Although we cannot exclude the possibility that these axons become myelinated farther along their path, they likely represent unmyelinated axons found in the corpus callosum(12). Interestingly, these three profiles of myelination can be found in neurons located in immediately adjacent positions within the same cortical layer (Fig. 2C).

To determine whether defined structural features are present along the unmyelinated segments of the layer II/III neurons that we traced, we examined them for the presence of synapses. We found that both afferent and efferent synapses exist on these unmyelinated tracts, including those of neurons with intermittent myelin (Fig. 2B, Fig. S5 and Table S2). Together, these features may provide a structural template for enhanced cortical plasticity.

In the peripheral nervous system, myelination is correlated with axon caliber(1, 2). Although in the CNS this correlation is less stringent, because diameters of myelinated and unmyelinated axons overlap(2), nevertheless axonal caliber may affect the myelin patterns that we observed. To investigate this possibility we reconstructed the volumes of 283 cell bodies of pyramidal neurons across all layers of the S1 dataset (Fig. 3A). We used these volumetric measurements as the most reliable indicator of average axon caliber, which is

correlated with soma size(13, 14). All pyramidal neurons in layers II/III, IV and VI had comparable sizes (layer II/III, 1654.3±38.6 μm^3, n=70; layer IV, 1712.1±44.4 μm^3, n=75; layer VI, 1592.2±40.5 μm^3, n=54, mean±s.e.m., Fig. 3A). Layer V contained pyramidal neurons of different sizes, including large size neurons likely representing subcerebral projection neurons (average volume= 2277.1±82.4 μm^3, n=82, mean±s.e.m., Fig. 3A). Despite different soma volumes, all neurons traced in layer V had comparable profiles of myelination and PMAS lengths (Fig. S4 and Fig. 3A). We also performed volumetric measurements of all neurons reconstructed in the V1 dataset and found that they were all comparable in volume regardless of their myelination profiles ("long PMAS" neurons, 1229.8±110.7 μm^3; "unmyelinated" neurons, 1410.9±29.1 μm^3; "intermittent myelin" neurons, 1220.2±58 μm^3; mean±s.e.m., Fig. 3B). Thus, we observed no correlation between neuronal soma size (and thus axon caliber) and profile of myelination.

Another possible determinant of myelin distribution may relate to availability of mature oligodendrocytes (OLs) and oligodendrocyte progenitors (OPCs) around different neurons. We quantified the radial distribution of OPCs and OLs in the cortex. SOX10+ cells, which include both OLs and OPCs(15), were present in all layers (Fig. 3C). Thus, we quantified the distribution of OPCs and OLs, separately. We found no difference in the radial distribution of OPCs, labeled by *Pdgfra* (1) (Fig. 3C). This data indicate that OPCs are not prevented from populating the upper layers of the cortex. In contrast, mature OLs, which are marked by Proteolipid Protein 1 (*Plp1*) (1) and adenomatous polyposis coli (APC) (16), showed a radial distribution that matched the myelin gradient, with the vast majority residing in the deep layers (Fig. 3C). Our results indicate that the observed layer-specific differences in myelination are not due to the absence of OPCs in the upper layers, but rather to their lamina-specific capacity to generate mature OLs.

OL development and myelin biogenesis are influenced by neuron-derived signals(17–20). Thus, the observed laminar differences in OPCs ability to give rise to OLs suggest influence of different neurons on OL development, and points to a role of neuronal diversity in modulating myelin distribution in different layers. To test this possibility, we investigated how misplacement of pyramidal neurons into different layers affects myelination of the cortex using two models of aberrant neuronal migration, Dab1−/− (21) and Emx1-Cre;RhoA^fl/fl mice (22). In the neocortex of the Dab1−/− mice, the radial position of pyramidal neurons is nearly inverted, with neurons of layers V and VI (labeled by CTIP2(6)) ectopically located in the upper layers and those of upper layers (labeled by CUX1) located in the deep layers(21, 23, 24). In this mutant cortex, the gradient of myelination was lost, and comparable levels of myelin (labeled by MBP and Black Gold II) were detected in all layers (Fig. 4B). This altered myelination profile was reflected in the even distribution of APC+ OLs in all layers of the mutant cortex (Fig. 4B). As the class-specific identity of pyramidal neurons in these mice is not affected(25), our results suggest that different classes of pyramidal neurons are endowed with different abilities to affect OL distribution and myelination. To further investigate this possibility we sought to determine whether a focal alteration in pyramidal neuron position, rather than the global change present in the Dab1−/− cortex, affected myelination. In the Emx1-Cre;RhoA^fl/fl mice, defects in the radial glia cytoskeleton result in the generation of a secondary cortical tissue, called subcortical band

heterotopia (SBH), which develops underneath a thinner neocortex (normocortex)(22). This model presents two types of focal abnormalities. First, SBH is mostly constituted by CUX1$^+$ upper layer pyramidal neurons with only scattered CTIP2$^+$ neurons (Fig. 4C). Second, heterotopias composed of deep layer neurons located within the upper layers can be found in the mutant normocortex(22). In both the SBH and the cortical heterotopias, we observed association between the presence of CTIP2$^+$ deep layer neurons and the ectopic distribution of APC$^+$ OLs and myelin (Fig. 4C). Thus changes in the laminar composition of pyramidal neurons affect the distribution of myelinating OLs, and pyramidal neurons of the upper and deep layers differentially influence myelin formation.

Here, we describe myelin distribution along single axons in the murine brain. We demonstrate that pyramidal neurons of different neocortical layers present signature profiles of myelination indicating that longitudinal myelin deposition is a defining feature of each neuron. This contributes to the emergence of a myelin gradient that reflects idiosyncratic interactions between pyramidal neurons and oligodendrocytes.

While the functional significance of these heterogeneous profiles of myelination awaits future elucidation, we propose that it may have served the evolutionary expansion and diversification of the neocortex, enabling the generation of different arrays of communication mechanisms and the emergence of highly complex neuronal behaviors.

Supplementary Material

Refer to Web version on PubMed Central for supplementary material.

Acknowledgments

References

1. Baumann N, Pham-Dinh D. Physiol Rev. 2001; 81:871. [PubMed: 11274346]

2. Hildebrand C, Remahl S, Persson H, Bjartmar C. Prog Neurobiol. 1993; 40:319. [PubMed: 8441812]

3. Helmstaedter M, et al. Nature. 2013; 500:168. [PubMed: 23925239]

4. Lichtman JW, Denk W. Science. 2011; 334:618. [PubMed: 22053041]

5. Ramón y Cajal, S. History of neuroscience. Oxford University Press; New York: 1995. Histology of the nervous system of man and vertebrates.

6. Molyneaux BJ, Arlotta P, Menezes JR, Macklis JD. Nat Rev Neurosci. 2007; 8:427. [PubMed: 17514196]

7. Nieto M, et al. J Comp Neurol. 2004; 479:168. [PubMed: 15452856]

8. Fairen A, Peters A, Saldanha J. J Neurocytol. 1977; 6:311. [PubMed: 71343]

9. Bock DD, et al. Nature. 2011; 471:177. [PubMed: 21390124]

10. Cardona A, et al. PLoS One. 2012; 7:e38011. [PubMed: 22723842]

11. Molyneaux BJ, et al. J Neurosci. 2009; 29:12343. [PubMed: 19793993]

12. Sturrock RR. Neuropathol Appl Neurobiol. 1980; 6:415. [PubMed: 7453945]

13. Sloper JJ, Powell TP. Philos Trans R Soc Lond B Biol Sci. 1979; 285:173. [PubMed: 88058]

14. Sloper JJ, Powell TP. Philos Trans R Soc Lond B Biol Sci. 1979; 285:124. [PubMed: 36637]

15. Kuhlbrodt K, Herbarth B, Sock E, Hermans-Borgmeyer I, Wegner M. J Neurosci. 1998; 18:237. [PubMed: 9412504]

16. Lang J, et al. J Neurosci. 2013; 33:3113. [PubMed: 23407966]

17. Wake H, Lee PR, Fields RD. Science. 2011; 333:1647. [PubMed: 21817014]

18. Barres BA, Raff MC. J Cell Biol. 1999; 147:1123. [PubMed: 10601327]

19. Michailov GV, et al. Science. 2004; 304:700. [PubMed: 15044753]

20. Taveggia C, Feltri ML, Wrabetz L. Nat Rev Neurol. 2010; 6:276. [PubMed: 20404842]

21. Sweet HO, Bronson RT, Johnson KR, Cook SA, Davisson MT. Mamm Genome. 1996; 7:798. [PubMed: 8875886]

22. Cappello S, et al. Neuron. 2012; 73:911. [PubMed: 22405202]

23. Ware ML, et al. Neuron. 1997; 19:239. [PubMed: 9292716]

24. Howell BW, Hawkes R, Soriano P, Cooper JA. Nature. 1997; 389:733. [PubMed: 9338785]

25. Tissir F, Goffinet AM. Nat Rev Neurosci. 2003; 4:496. [PubMed: 12778121]

26. Tapia JC, et al. Nat Protoc. 2012; 7:193. [PubMed: 22240582]

27. Hayworth KJ, Kasthuri N, Schalek R, Lichtman JW. Microsc Microanal. 2006; 12:86.

28. Terasaki M, et al. Cell. 2013; 154:285. [PubMed: 23870120]

29. Kasthuri, N., et al. Society for Neuroscience; Chicago, IL. Oct 17–21, 2009;

30. Arlotta P, et al. Neuron. 2005; 45:207. [PubMed: 15664173]

31. Lodato S, et al. Neuron. 2011; 69:763. [PubMed: 21338885]

32. Gallyas F. Neurol Res. 1979; 1:203. [PubMed: 95356]

33. Innocenti GM, Vercelli A, Caminiti R. Cereb Cortex. 2013
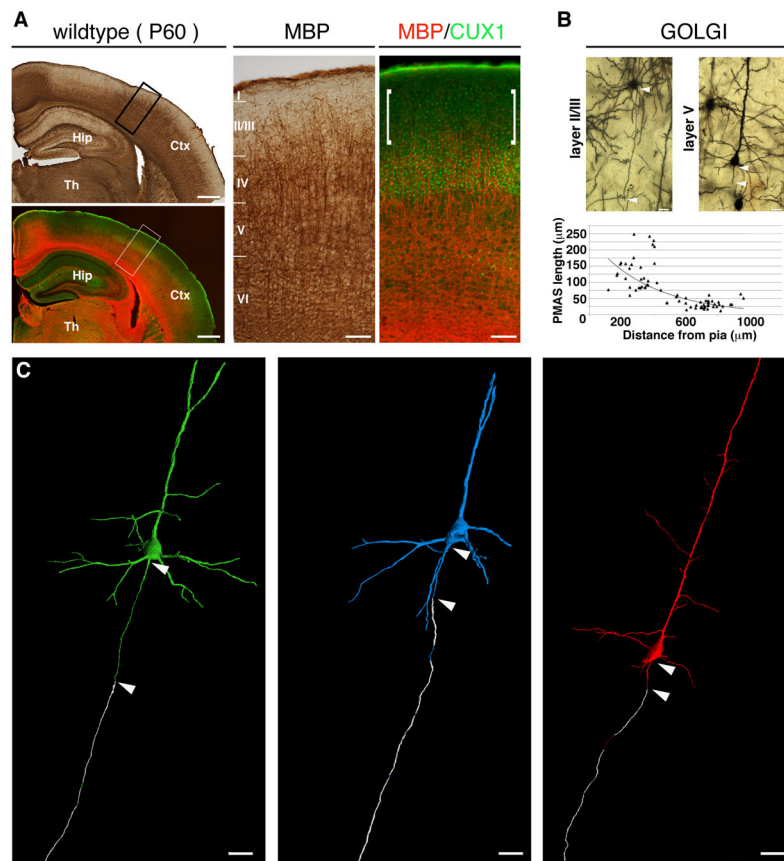
**Fig. 1. Radial distribution of myelin in the adult mouse neocortex**
(**A**) Immunohistochemical staining of MBP and CUX1 in coronal sections of wild type adult neocortex. High magnifications of boxed areas show reduced levels of myelin in layer II/III (brackets). (**B**) PMAS lengths (arrowheads) in Golgi-Cox-labeled adult wild type cortex. Top, representative neurons in layer II/III and layer V. Bottom, scatter plot of PMAS length versus distance of neuronal cell bodies from the pia (n=72, R^2= 0.61093). (**C**) 3D renderings of three representative neurons. The green and blue neurons were located in layer III–IV and the red neuron was in layer V. Myelin is shown in white. Ctx, cortex; Hip, hippocampus, Th, thalamus. Scale bars, 500 μm (**A**, low magnification), 100 μm (**A**, insets), 20 μm (**B**), 25 μm (**C**).
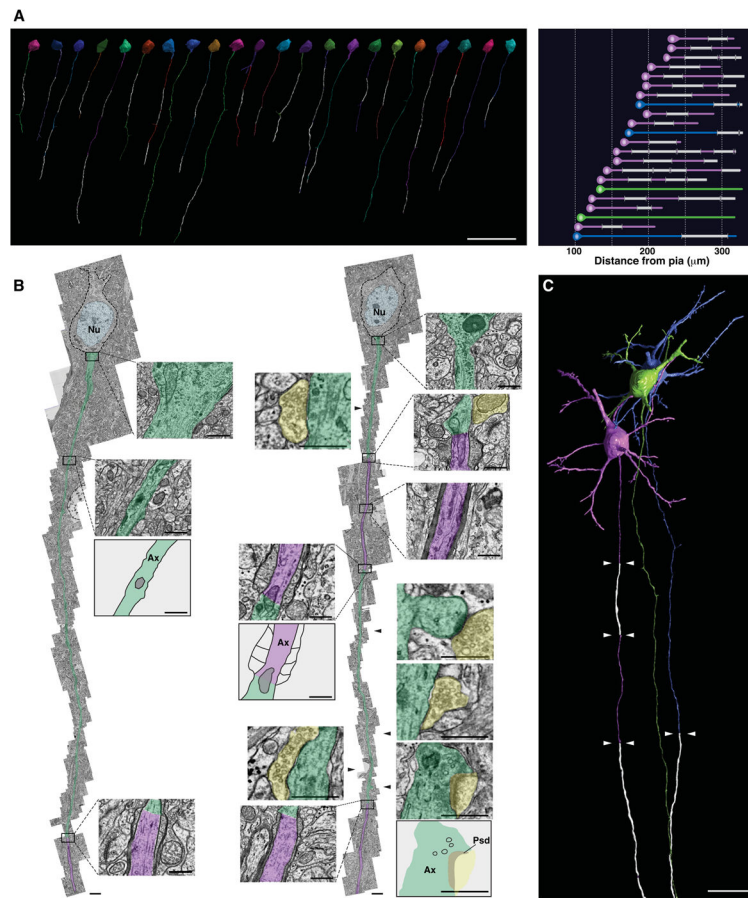
Fig. 2. Layer II/III pyramidal neurons display novel profiles of longitudinal myelination including intermittent myelin

(**A**) High-resolution rendering of myelin distribution along single axons of 22 pyramidal neurons traced and reconstructed in layer II/III of the V1 dataset. Right panel, soma position and lengths of axonal tracts for all neurons rendered in left panel. Magenta, neurons with intermittent myelin; blue, neurons with long PMAS; green, neurons with unmyelinated axons; white, myelinated axonal segments. (**B**) Representative, serial EM reconstructions of neurons with long PMAS (left) or intermittent myelin (right). Unmyelinated axon tracts are highlighted in green and myelinated tracts in magenta. Insets, EM images and schematic representations of selected regions from each axon. Yellow, selected synapses mapped on the intermittently myelinated axon. Ax, axon; Nu, nucleus, Psd, post-synaptic density. (**C**) High-resolution rendering of three representative neurons displaying different myelination modes. Native positions of these neurons are preserved in the rendering. Arrowheads mark the boundaries of myelinated tracts (white). Scale bars, 50 μm (**A**), 2 μm (**B**), 0.5 μm (**B**, insets), 20 μm (**C**).
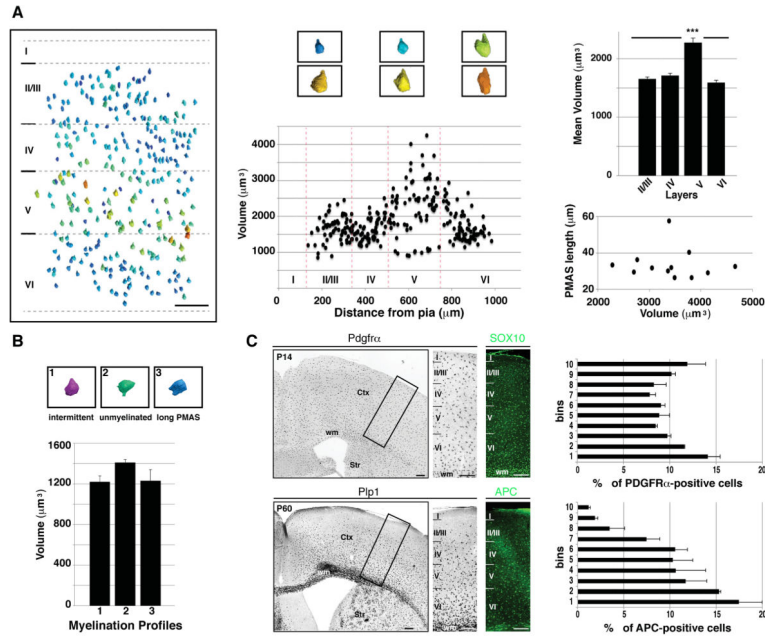
Fig. 3. Longitudinal myelination profile is independent of neuron size and availability of oligodendrocyte progenitors

(A) Rendering and volumetric measurements of 283 pyramidal neurons across all layers of the S1 dataset. Soma size is color-coded with largest and smallest neurons rendered in orange and blue, respectively. Center, scatter plot of soma volumes versus distances from the pia. Top right, average values of the soma volumes measured in each cortical layer. Bottom right, scatter plot of PMAS lengths in layer V and VI versus cell body volumes. **(B)** Average values of soma volumes of 22 neurons from the V1 dataset, grouped according to their myelination profiles. **(C)** Top, immunohistochemistry for SOX10 and *in situ* hybridization for *Pdgfrα* in P14 wild type cortex. Right, quantification of OPCs distribution across layers. Bottom, *in situ* hybridization for *Plp1* and immunohistochemistry for APC in adult wild type cortex. Right, quantification of OL distribution across layers. Error bars, mean±s.e.m. Ctx, cortex; wm, white matter; Str, striatum. Scale bars, 150 μm (**A**), 200 μm (**C**).
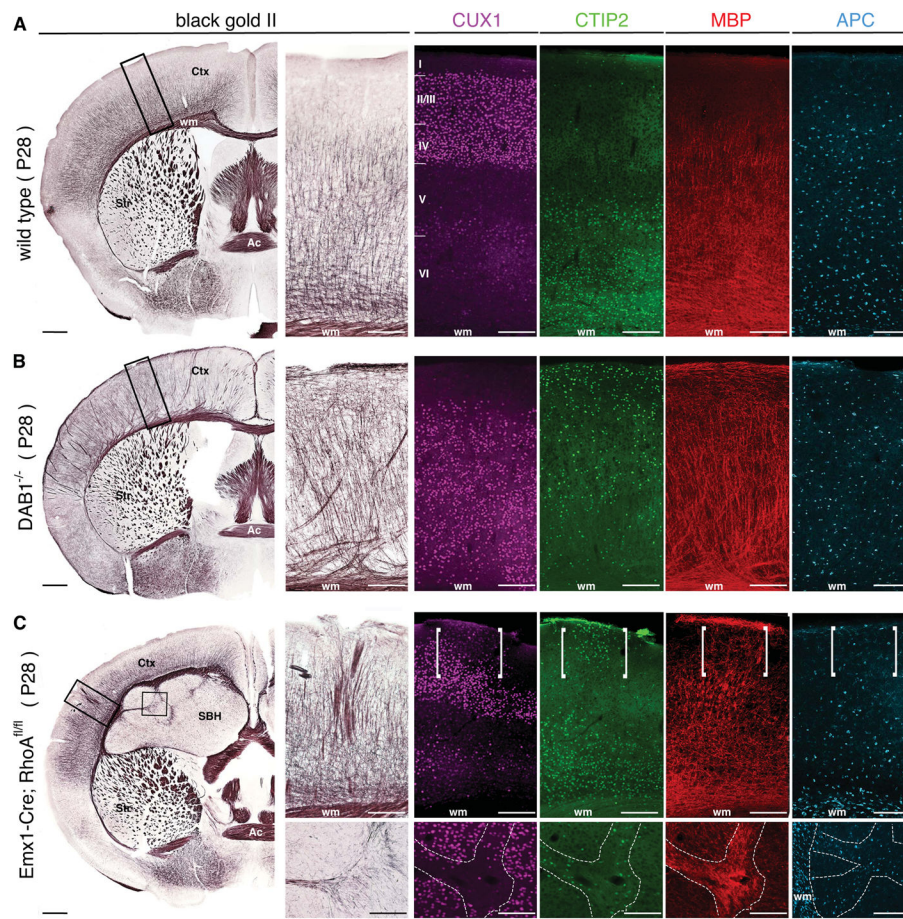
Fig. 4. Distribution of myelin depends on the laminar position of distinct classes of projection neurons
Histological staining of myelin by Black Gold (BG) II and immunohistochemistry for CUX1, CTIP2, MBP and APC in P28 cortex of wild type (**A**), Dab1^{−/−} (**B**) and Emx1-Cre;RhoA^{fl/fl} (**C**) mice. Immunohistochemistry for APC is on immediately consecutive sections. (**C**) Upper insets, deep layer neuron heterotopias and myelin distribution in normocortex. Lower insets, myelin deposition in the SBH. Ac, anterior commissure; Ctx, cortex; SBH, subcortical band heterotopia; Str, striatum; wm, white matter. Scale bars, 400 μm (**A–C**, lower magnification panels), 200 μm (**A–C**, insets).